TABLE 1. Characteristics of patients with CR associated with antiviral therapy

Patient	1	2	3	4	5	6	7
Age (years)	62	41	45	67	50	59	49
Gender	Female	Male	Female	Female	Female	Male	Male
ABO mismatch with donor	Match	Match	Match	Mismatch	Match	Mismatch	Match
Relation to donor	Related	Related	Nonrelated	Related	Nonrelated	Nonrelated	Nonrelated
Graft type (lobe)	Right	Right	Right	Right	Left	Right	Right
Splenectomy	No	No	No	No	Yes	Yes	No
Previous ACR	Yes	Yes	Yes	No	Yes	No	No
Previous moderate/severe ACR	Yes	No	Yes	No	Yes	No	No
Previous steroid pulse	Yes	No	No	No	Yes	No	No
HCV genotype	1b	1b	1b	2a	1b	1b	1b
HCV RNA (kIU/mL) before IFN	>850	3620	1790	>5000	<5000	<5000	16,000
METAVIR score before IFN	A2 F2	A2 F0	A1 F0	A1 F1	A2 F1	A1 F0	A1 F1
Months from LT to IFN	13	2	5	13	7	9	72
Months from initiation of IFN to diagnosis of CR	9	1	16	10	15	8	7
Immunosuppressant at initiation of IFN	Tacrolimus	Tacrolimus,	Tacrolimus, MMF	Tacrolimus, MMF, PSL	Cyclosporine, MMF	Tacrolimus, MMF	MMF
Trough level of CNI	7.8	7.9	7.9	6.8	152	5.9	—
Reduction of immunosuppressant during IFN (reduced drugs)	No	Yes (tacrolimus)	Yes (tacrolimus, MMF)	Yes (MMF, PSL)	Yes (MMF)	No	Yes (MMF)
Type of IFN	Standard	Standard	Standard	Pegylated	Pegylated	Pegylated	Pegylated
Ribavirin discontinuation	No	No	Yes	Yes	No	No	Yes
IFN at diagnosis of CR	On treatment	On treatment	1 month after end of IFN	5 months after end of IFN	On treatment	On treatment	On treatment
At diagnosis of CR							
Liver biopsy	Foam cell arteriopathy, bile duct atrophy	Bile duct atrophy	Bile duct atrophy	Bile duct atrophy, bile duct loss	Bile duct atrophy, bile duct loss	Bile duct atrophy, bile duct loss	Foam cell arteriopathy, bile duct atrophy
AST (IU/L)	121	90	53	73	331	124	36
ALT (IU/L)	67	37	43	63	288	52	32
ALP (IU/L)	2034	906	494	1751	2143	528	1164
γ-GTP (IU/L)	561	768	155	209	515	27	1489
Bilirubin (mg/dL)	18.6	18.8	31.5	38.1	11.8	16.4	22.6
HCV RNA (kIU/mL)	Undetectable	460	Undetectable	Undetectable	16,000	Undetectable	0.40
Treatment for CR	Tacrolimus, MMF	Tacrolimus	Tacrolimus, steroid pulse, MMF	Tacrolimus, MMF, PSL	Tacrolimus, MMF, rapamycin, steroid pulse	Tacrolimus, steroid pulse, MMF	Tacrolimus, MMF, rapamycin, steroid pulse
Outcome	Died	Alive	Died	Died	Died	Died	Died
Months from diagnosis of CR to death	64	—	1	1	1	3	1

ALT, alanine aminotransferase; AST, aspartate aminotransferase; PSL, prednisolone.

with CR after antiviral therapy was terminated. Antiviral therapy was discontinued in the remaining five patients. Of note, six patients were treated with IFN for more than 7 months, suggesting that long-term administration of IFN is associated with CR. Liver biopsy was performed for diagnosis of CR because of abnormal liver function tests in all cases. All patients with documented CR had high levels of alkaline phosphatase (ALP). Total bilirubin levels were extremely high (11.8–38.1 mg/dL) at diagnosis, suggesting a delayed diagnosis of CR. All liver biopsies showed atrophy affecting most bile ducts as well as hepatocanalicular cholestasis. Two patients (patients 1 and 7) showed foam cell obliterative arteriopathy. Bile duct loss was shown in 100%, 67%, and 20% of the portal tracts in patients 4, 5, and 6, respectively. In none of the seven patients was evidence of ACR found in the biopsy specimens. Hepatic artery or biliary tract obstruction or structuring was excluded by imaging in all patients.

Serum HCV RNA was undetectable in four patients at CR diagnosis and remained undetectable in all four patients during the follow-up period. Two of the four patients were considered to have SVR. Final outcomes could not be determined in the remaining two patients who died within 24 weeks after termination of treatment.

Various intensive treatment protocols were used for these seven patients after CR diagnosis, including increase of tacrolimus dose, addition or increase in MMF and/or prednisolone dose, administration of steroid pulse therapy, and inclusion of rapamycin in the therapy. CR progressed rapidly to liver failure in five patients (patients 3–7). These five patients died within 3 months after diagnosis of CR due to liver failure and infection. The liver damage in patient 1 gradually progressed to liver failure, and the patient died at 64 months after CR was diagnosed. Only one patient (patient 2) recovered from CR and survived, although a follow-up liver biopsy showed chronic hepatitis C.

Risk Factors of CR Associated with Antiviral Therapy

Factors associated with the development of CR during and after antiviral therapy were analyzed by comparing the features of 7 CR patients with those of 76 patients who did not develop CR despite receiving antiviral therapy for more than 1 year (Table 2). A reduction of the immunosuppressant dose during antiviral therapy (P=0.034) and a low fibrosis stage before antiviral therapy (P=0.045) were significantly associated with antiviral therapy-related CR. No significant associations were found with other variables, including donor factors, ribavirin discontinuation, and undetectable HCV RNA. The rate of previous ACR (P=0.065), rate of previous moderate or severe ACR (P=0.059), ALP level (P=0.121), and γ-glutamyl transpeptidase (γ-GTP) level (P=0.051) before antiviral therapy was higher in the patients who developed CR, but the differences from patients without CR were not significant.

DISCUSSION

Of the 125 patients, 7 (6%) who received antiviral therapy for hepatitis C after LDLT developed CR. CR progressed rapidly, resulting in death within 3 months after diagnosis, in 5 of these 7 patients.

The risk of rejection have been suggested to increase with IFN administration because of the drug's theoretical immunomodulatory actions, such as up-regulation of human leukocyte antigen class II antigens and induction of proinflammatory cytokines (*21*). Previous studies have reported that the frequency of CR in patients who received IFN was substantially higher compared with patients who did not receive antiviral therapy (*11, 12, 17*). In the present study, the rate of antiviral therapy-associated CR was 6%. This rate is high, because no CR occurred in the entire study period other than during or within 6 months after termination of antiviral therapy in the 230 HCV-positive recipients analyzed. Some cases showed sudden onset of CR after a long transplantation period in the absence of preexisting ACR, supporting the association of antiviral therapy with CR.

In our analysis, the two significant risk factors for CR were reduction of the immunosuppressant dose during antiviral therapy and low fibrosis score at antiviral therapy initiation. Additional characteristics associated with CR were elevated cholestatic enzyme levels at the time of diagnosis, onset of CR more than 7 months after treatment initiation (excluding one patient) and poor prognosis after the diagnosis. The MMF dose was reduced or stopped during antiviral therapy in four of five patients who had received MMF at the start of the treatment. We had initially tried to reduce the MMF dose during antiviral therapy, because MMF is known to suppress the bone marrow and could therefore augment the cytopenic effects of IFN and ribavirin. We had reduced immunosuppressant according to our reduction protocol even during antiviral therapy. Based on the data, we subsequently changed our strategy to maintaining the MMF dose and increasing the trough level of CNIs during antiviral therapy. The reason for the association between the low fibrosis score and CR is currently unclear. Although some institutions recommend early introduction of antiviral therapy (*8, 9*), our data suggest that antiviral therapy should not be administered to patients with no or mild fibrosis. On the contrary, it is reported that tolerance to therapy decreases significantly in patients with a fibrosis stage ≥3 on baseline liver biopsy (*22*). Therefore, the antiviral therapy should be initiated in patients with a fibrosis stage 2, as the recent review articles recommended (*23, 24*).

All our patients underwent LDLT, but no characteristics specific to LDLT, including blood-relative donors, graft size, and ABO incompatibility, were identified as risk factors for CR in our study. This appears to indicate that LDLT and DDLT patients do not differ with respect to antiviral therapy-associated CR.

Early diagnosis of CR, as well as prevention, is important for ensuring improved outcomes in LT recipients. CR was diagnosed in our patients after liver damage had already progressed. Histologic diagnosis of CR was difficult in all these cases, despite repeated liver biopsy examination. However, all the patients had elevated ALP and γ-GTP levels before jaundice was observed. CR should therefore be suspected when a cholestatic liver enzyme pattern develops during antiviral therapy for hepatitis C. When imaging has excluded large bile duct and/or hepatic artery changes as the

TABLE 2. Risk factors for CR

	CR (n=7)	No CR (n=76)	P
Age at LT (years)	50 (41−67)	56 (36−69)	0.506[a]
Gender, male/female	3/4	44/32	0.352[b]
HCV genotype, 1/non-1	6/1	71/5	0.421[b]
Donor age at LT (years)	46 (28−60)	42 (21−65)	0.857[a]
Donor gender, male/female	4/3	40/36	0.568[b]
Sex mismatch, match/mismatch	0/7	26/50	0.064[b]
ABO mismatch, match/mismatch	5/2	59/17	0.507[b]
Relation to donor, related/nonrelated	3/4	48/28	0.254[b]
HLA-A matched number, 0/1/2/unknown	0/5/2/0	13/44/16/3	0.332[a]
HLA-B matched number, 0/1/2/unknown	2/4/1/0	21/47/5/3	0.778[a]
HLA-DR matched number, 0/1/2/unknown	3/3/1/0	18/47/8/3	0.487[a]
Graft type, left lobe/right lobe	1/6	9/67	0.608[b]
Splenectomy, yes/no	2/5	38/38	0.247[b]
Previous ACR, yes/no	4/3	17/59	0.065[b]
Previous moderate/severe ACR, yes/no	3/4	9/67	0.059[b]
Previous steroid pulse therapy, yes/no	2/5	8/68	0.198[b]
Months from LT to therapy	9.0 (1.8−72.4)	9.1 (2.2−68.8)	0.694[a]
Valuables at initiation of IFN			
Age (years)	55 (41−68)	57 (37−70)	0.599[a]
CNI tacrolimus/cyclosporine	5/1	71/5	0.376[b]
Trough level for tacrolimus (ng/mL)	7.3 (0−7.9)	6.2 (2.6−10.9)	0.641[a]
AST (IU/L)	68 (24−464)	76 (21−331)	0.908[a]
ALT (IU/L)	88 (25−354)	79 (20−392)	0.842[a]
ALP (IU/L)	878 (283−2977)	462 (168−2818)	0.121[a]
γ-GTP (IU/L)	317 (48−1623)	112 (15−1704)	0.051[a]
Bilirubin (mg/dL)	0.8 (0.3−10.4)	0.9 (0.3−4.6)	0.861[a]
Activity grade, A1/A2/A3	4/3/0	50/24/2	0.693[a]
Fibrosis stage, F0/F1/F2/F3	3/3/1/0	4/56/13/3	0.045[a]
Reduction of immunosuppressant during IFN, yes/no	5/2	22/54	0.034[b]
Ribavirin discontinuation during IFN, yes/no	3/4	26/50	0.468[b]
Undetectable HCV RNA during IFN, yes/no	4/3	51/25	0.439[b]

[a] Wilcoxon rank-sum test.
[b] Chi-square test.
Comparison was made between 7 patients with CR and 76 patients without CR despite receiving antiviral therapy for more than 1 year (No CR). Qualitative variables expressed as number. Quantitative variables expressed as median (range).
ALT, alanine aminotransferase; AST, aspartate aminotransferase; HLA, human leukocyte antigen.

potential etiology of abnormal liver function, we believe that cessation of antiviral therapy and initiation of intensive immunosuppressive therapy should be considered, even without histologic confirmation of CR.

Some limitations of this study are its retrospective nature and relatively small sample size. Because the frequency of CR was low, the sample size was not adequate for multivariate analysis.

In conclusion, CR developed in association with antiviral therapy for recurrent hepatitis C after LDLT. Reduction of the immunosuppressant dose during antiviral therapy should be avoided and antiviral therapy should not be administered to patients with no or mild fibrosis to prevent antiviral therapy-associated CR. Early CR diagnosis should be suspected when a cholestatic liver enzyme pattern develops during antiviral therapy. In these cases, discontinuation of antiviral therapy and increase in the immunosuppressant dose are recommended when other causes of liver dysfunction are excluded.

MATERIALS AND METHODS

Patients

A total of 232 patients with HCV-related end-stage liver disease underwent LDLT at Kyoto University Hospital between March 1999 and September 2012. Two patients who received a liver graft from an identical twin were excluded from this study, because they did not require immunosuppression because of genetic identity. Of the remaining 230 patients, 157 patients were followed up for more than 6 months after LDLT in our hospital. Antiviral therapy was administered to 125 of the 157 patients with recurrent hepatitis C between January 2001 and September 2012. They were diagnosed with recurrent hepatitis C after LDLT via serum HCV RNA analysis and histologic evidence. The remaining 32 patients did not receive antiviral therapy for various reasons: serum HCV RNA negative after LDLT (n=4), no histologic hepatitis C recurrence in the follow-up period (n=13),

no fibrosis seen by liver histology (n=8), and ongoing treatment for the other complications (n=7). CR was defined histologically according to the updated International Banff Schema for Liver Allograft Rejection with the following criteria: (a) the presence of bile duct atrophy/pyknosis affecting most of the bile ducts with or without bile duct loss, (b) convincing foam cell obliterative arteriopathy, or (c) bile duct loss affecting more than 50% of the portal tracts (*13*). Patients who were diagnosed with CR based on these diagnostic criteria during or within 6 months after terminating antiviral therapy were examined for antiviral therapy-associated CR. The clinical features of these 7 patients with CR were compared with those of 76 patients who did not have CR despite receiving antiviral therapy for more than 1 year to determine the risk factors for CR.

The study protocol was approved by the ethics committee at Kyoto University and performed in compliance with the Helsinki Declaration.

Treatment Protocol and Definition of Responses to Treatment

Between January 2001 and April 2004, 40 patients with recurrent hepatitis C after LDLT received treatment with IFN-α-2b plus ribavirin (*25*). From May 2004 to June 2011, patients received combination therapy with peg-IFN-α-2b plus ribavirin (*26*). Patients who acquired a negative serum HCV RNA status within 12 months after treatment initiation continued to receive the treatment for an additional 12 months. Patients who tested negative for serum HCV RNA for more than 6 months after completing IFN therapy were defined as having achieved SVR. For those who tested positive for serum HCV RNA after 12 months of treatment, therapy was discontinued or switched to maintenance therapy with low-dose peg-IFN (*27*), and patients were classified as having shown no response.

Histologic Assessment

Liver biopsy examination was performed when patients showed abnormal liver function tests, or at yearly intervals, with informed consent. Biopsy specimens were evaluated by two pathologists (H.H. and A.M.-H.) with extensive experience in the pathology of LT. Necroinflammatory activity (A0–A3) and fibrosis stage (F0–F4) were assessed using METAVIR scores (*28*).

Immunosuppression

Tacrolimus with low-dose steroid or MMF was administered to most patients for immunosuppression (*25*). The target whole blood lower level for tacrolimus was 10 to 15 ng/mL during the first 2 weeks, 10 ng/mL thereafter, and 5 to 8 ng/mL starting from the second month. Steroid therapy was initiated at a dose of 10 mg/kg methylprednisolone before graft reperfusion then tapered down from 1 mg/kg per day on days 1 to 3, to 0.5 mg/kg per day on days 4 to 6, and to 0.3 mg/kg per day on day 7. Subsequently, oral prednisolone was continued at 0.3 mg/kg per day until the end of the first month, and this was followed by 0.1 mg/kg per day until the end of the third month. After that, steroid administration was terminated. MMF was initiated at a starting dose of 10 to 15 mg/kg on day 1, which was gradually increased to a target dose of 30 mg/kg, and this was continued for 6 months. Thereafter, MMF administration was terminated. Four patients received cyclosporine microemulsions instead of tacrolimus. MMF and/or prednisolone was administered again to patients who experienced refractory rejection or required reduction of the tacrolimus or cyclosporine dose because of adverse events and then tapered down gradually. Twenty-seven patients who received ABO-incompatible transplants were treated with rituximab, plasma exchange, and hepatic artery or portal vein infusion with prostaglandin E1 and methylprednisolone (*29*).

Virologic Assays

HCV genotype was determined using a genotyping system based on polymerase chain reaction (PCR) to amplify the core region using genotype-specific primers (*30*). The serum HCV RNA load was evaluated before LDLT, before IFN treatment, once a month during treatment, and 24 weeks after treatment using PCR and an Amplicor HCV assay (Cobas Amplicor HCV Monitor; Roche Molecular Systems, Pleasanton, CA) until April 2008. A real-time PCR-based quantitation method for HCV (COBAS AmpliPrep/COBAS TaqMan HCV Test; Roche Molecular Systems) was used alternatively from May 2008.

Statistical Analysis

To evaluate the association between patient characteristics and CR, the characteristics were defined and compared between patients with and without CR. Medians and ranges were determined for continuous variables, and data were analyzed using the Wilcoxon rank-sum test. Categorical variables were expressed as counts, and data were analyzed using the chi-square test. A significance level of $P<0.05$ was considered significant. Statistical analyses were performed using PASW Statistics version 18.0.0 (SPSS, an IBM company).

REFERENCES

1. Berenguer M, Prieto M, San Juan F, et al. Contribution of donor age to the recent decrease in patient survival among HCV-infected liver transplant recipients. *Hepatology* 2002; 36: 202.
2. Feray C, Caccamo L, Alexander GJ, et al. European collaborative study on factors influencing outcome after liver transplantation for hepatitis C. European Concerted Action on Viral Hepatitis (EUROHEP) Group. *Gastroenterology* 1999; 117: 619.
3. Forman LM, Lewis JD, Berlin JA, et al. The association between hepatitis C infection and survival after orthotopic liver transplantation. *Gastroenterology* 2002; 122: 889.
4. Gane E. The natural history and outcome of liver transplantation in hepatitis C virus-infected recipients. *Liver Transpl* 2003; 9: S28.
5. Prieto M, Berenguer M, Rayon JM, et al. High incidence of allograft cirrhosis in hepatitis C virus genotype 1b infection following transplantation: relationship with rejection episodes. *Hepatology* 1999; 29: 250.
6. Sanchez-Fueyo A, Restrepo JC, Quinto L, et al. Impact of the recurrence of hepatitis C virus infection after liver transplantation on the long-term viability of the graft. *Transplantation* 2002; 73: 56.
7. Velidedeoglu E, Mange KC, Frank A, et al. Factors differentially correlated with the outcome of liver transplantation in HCV+ and HCV- recipients. *Transplantation* 2004; 77: 1834.
8. Gordon FD, Kwo P, Vargas HE. Treatment of hepatitis C in liver transplant recipients. *Liver Transpl* 2009; 15: 126.
9. Terrault NA. Hepatitis C therapy before and after liver transplantation. *Liver Transpl* 2008; 14: S58.
10. Berenguer M. Systematic review of the treatment of established recurrent hepatitis C with pegylated interferon in combination with ribavirin. *J Hepatol* 2008; 49: 274.
11. Fernandez I, Ulloa E, Colina F, et al. Incidence, risk factors, and outcome of chronic rejection during antiviral therapy for post-transplant recurrent hepatitis C. *Liver Transpl* 2009; 15: 948.
12. Stanca CM, Fiel MI, Kontorinis N, et al. Chronic ductopenic rejection in patients with recurrent hepatitis C virus treated with pegylated interferon alfa-2a and ribavirin. *Transplantation* 2007; 84: 180.
13. Demetris A, Adams D, Bellamy C, et al. Update of the International Banff Schema for Liver Allograft Rejection: working recommendations for the histopathologic staging and reporting of chronic rejection. An International Panel. *Hepatology* 2000; 31: 792.
14. Demetris AJ. Distinguishing between recurrent primary sclerosing cholangitis and chronic rejection. *Liver Transpl* 2006; 12: S68.
15. O'Grady J. The immunoreactive patient: rejection and autoimmune disease. *Liver Transpl* 2011; 17: S29.
16. O'Leary JG, Kaneku H, Susskind BM, et al. High mean fluorescence intensity donor-specific anti-HLA antibodies associated with chronic rejection postliver transplant. *Am J Transplant* 2011; 11: 1868.
17. Berenguer M, Palau A, Fernandez A, et al. Efficacy, predictors of response, and potential risks associated with antiviral therapy in liver transplant recipients with recurrent hepatitis C. *Liver Transpl* 2006; 12: 1067.
18. Dousset B, Conti F, Houssin D, et al. Acute vanishing bile duct syndrome after interferon therapy for recurrent HCV infection in liver-transplant recipients. *N Engl J Med* 1994; 330: 1160.
19. Feray C, Samuel D, Gigou M, et al. An open trial of interferon alfa recombinant for hepatitis C after liver transplantation: antiviral effects and risk of rejection. *Hepatology* 1995; 22: 1084.

20. Stravitz RT, Shiffman ML, Sanyal AJ, et al. Effects of interferon treatment on liver histology and allograft rejection in patients with recurrent hepatitis C following liver transplantation. *Liver Transpl* 2004; 10: 850.
21. Selzner N, Guindi M, Renner EL, et al. Immune-mediated complications of the graft in interferon-treated hepatitis C positive liver transplant recipients. *J Hepatol* 2011; 55: 207.
22. Roche B, Sebagh M, Canfora ML, et al. Hepatitis C virus therapy in liver transplant recipients: response predictors, effect on fibrosis progression, and importance of the initial stage of fibrosis. *Liver Transpl* 2008; 14: 1766.
23. Berenguer M, Schuppan D. Progression of liver fibrosis in post-transplant hepatitis C: mechanisms, assessment and treatment. *J Hepatol* 2013; 58: 1028.
24. Coilly A, Roche B, Samuel D. Current management and perspectives for HCV recurrence after liver transplantation. *Liver Int* 2013; 33: 56.
25. Ueda Y, Takada Y, Haga H, et al. Limited benefit of biochemical response to combination therapy for patients with recurrent hepatitis C after living-donor liver transplantation. *Transplantation* 2008; 85: 855.
26. Ueda Y, Takada Y, Marusawa H, et al. Individualized extension of pegylated interferon plus ribavirin therapy for recurrent hepatitis C genotype 1b after living-donor liver transplantation. *Transplantation* 2010; 90: 661.
27. Ueda Y, Marusawa H, Kaido T, et al. Effect of maintenance therapy with low-dose peginterferon for recurrent hepatitis C after living donor liver transplantation. *J Viral Hepat* 2012; 19: 32.
28. Bedossa P, Poynard T. An algorithm for the grading of activity in chronic hepatitis C. The METAVIR Cooperative Study Group. *Hepatology* 1996; 24: 289.
29. Raut V, Mori A, Kaido T, et al. Splenectomy does not offer immunological benefits in ABO-incompatible liver transplantation with a preoperative rituximab. *Transplantation* 2012; 93: 99.
30. Ohno O, Mizokami M, Wu RR, et al. New hepatitis C virus (HCV) genotyping system that allows for identification of HCV genotypes 1a, 1b, 2a, 2b, 3a, 3b, 4, 5a, and 6a. *J Clin Microbiol* 1997; 35: 201.

IJC
International Journal of Cancer

A model of liver carcinogenesis originating from hepatic progenitor cells with accumulation of genetic alterations

Soo Ki Kim[1], Akihiro Nasu[1], Junji Komori[2], Takahiro Shimizu[1], Yuko Matsumoto[1], Yasuko Minaki[1], Kenji Kohno[3], Kazuharu Shimizu[4], Shinji Uemoto[2], Tsutomu Chiba[1] and Hiroyuki Marusawa[1]

[1] Department of Gastroenterology and Hepatology, Graduate School of Medicine, Kyoto University, Kyoto, Japan
[2] Department of Surgery, Graduate School of Medicine, Kyoto University, Kyoto, Japan
[3] Graduate School of Biological Sciences, Nara Institute of Science and Technology, Nara, Japan
[4] Department of Nanobio Drug Discovery, Graduate School of Pharmaceutical Sciences, Kyoto University, Kyoto, Japan

Activation-induced cytidine deaminase (AID) contributes to inflammation-associated carcinogenesis through its mutagenic activity. In our study, by taking advantage of the ability of AID to induce genetic aberrations, we investigated whether liver cancer originates from hepatic stem/progenitor cells that accumulate stepwise genetic alterations. For this purpose, hepatic progenitor cells enriched from the fetal liver of AID transgenic (Tg) mice were transplanted into recipient "toxin-receptor mediated conditional cell knockout" (TRECK) mice, which have enhanced liver regeneration activity under the condition of diphtheria toxin treatment. Whole exome sequencing was used to determine the landscape of the accumulated genetic alterations in the transplanted progenitor cells during tumorigenesis. Liver tumors developed in 7 of 11 (63.6%) recipient TRECK mice receiving enriched hepatic progenitor cells from AID Tg mice, while no tumorigenesis was observed in TRECK mice receiving hepatic progenitor cells of wild-type mice. Histologic examination revealed that the tumors showed characteristics of hepatocellular carcinoma and partial features of cholangiocarcinoma with expression of the AID transgene. Whole exome sequencing revealed that several dozen genes acquired single nucleotide variants in tumor tissues originating from the transplanted hepatic progenitor cells of AID Tg mice. Microarray analyses revealed that the majority of the mutations (>80%) were present in actively transcribed genes in the liver-lineage cells. These findings provided the evidence suggesting that accumulation of genetic alterations in fetal hepatic progenitor cells progressed to liver cancers, and the selection of mutagenesis depends on active transcription in the liver-lineage cells.

Tumorigenesis comprises multiple processes with a stepwise accumulation of genetic alterations that drive the progressive transformation of normal cells into highly malignant derivatives.[1] Recent studies of a large number of genomes in human cancer tissues clarified that cancer cells generally possess hundreds of somatic mutations and dysregulated gene expression profiles.[2–4] Although the origin of cancer cells remains mostly unsolved at present, it might be difficult for fully differentiated cells to acquire these large numbers of nucleotide alterations during their limited life-span to achieve malignant transformation. In contrast, stem/progenitor cells have a long lifetime to supply the differentiated progenies in each organ. Thus, it appears reasonable to assume that long-lived tissue stem/progenitor cells can accumulate genetic alterations and hence could be the origin of tumor cells. Consistent with this hypothesis, a number of studies have provided evidence that the mutations would most likely result in expansion of the altered stem cells, perpetuating and

Key words: liver cancer, hepatic progenitor cells, activation-induced cytidine deaminase (AID), mutation, liver carcinogenesis

Abbreviations: AFP: alpha-fetoprotein: AID: activation-induced cytidine deaminase; hHB-EGF: human heparin binding epidermal growth factor-like growth factor: CK: cytokeratin; DT: diphtheria toxin: GFP: green fluorescent protein; HCC: hepatocellular carcinoma: ICC: intrahepatic cholangiocarcinoma; MAPK: mitogen-activated protein kinase: PPAR: peroxisome proliferator-activated receptor; PCR: polymerase chain reaction: SNV: single nucleotide variant; Tg: transgenic: TRECK: toxin-receptor mediated conditional cell knockout

Additional Supporting Information may be found in the online version of this article.

S.K.K. and A.N. contributed equally to this work.

Grant sponsor: JSPS KAKENHI, Research program of the Project for Development of Innovative Research on Cancer Therapeutics (P-Direct) from Ministry of Education, Culture, Sports, Science and Technology of Japan, Health and Labour Sciences Research Grants for Research from the Ministry of Health, Labour and Welfare, and Takeda Science Foundation

DOI: 10.1002/ijc.28445

History: Received 7 Mar 2013; Accepted 7 Aug 2013; Online 19 Aug 2013

Correspondence to: Hiroyuki Marusawa, Department of Gastroenterology and Hepatology, Graduate School of Medicine, Kyoto University, Kyoto, Japan, Tel.: +81-75-751-4319, Fax: +81-75-751-4303, E-mail: maru@kuhp.kyoto-u.ac.jp

What's new?

The accumulation of stepwise genetic aberrations is a defining feature of cancer. To better understand this process in liver cancer, the present study leveraged the mutagenic ability of activation-induced cytidine deaminase (AID) by using fetal hepatic progenitor cells from AID transgenic mice. The progenitor cells were transplanted into "toxin-receptor mediated conditional cell knockout" mice, where they accumulated genetic alterations sufficient to induce liver tumor formation, for both HCC and cholangiocarcinoma. The landscape of accumulated alterations was revealed by whole exome sequencing. The findings lend support to the idea that cancer arises from tissue stem/progenitor cells.

increasing the chances of additional mutations, leading to malignant transformation.[5–8]

Several studies have provided evidence that hepatocellular carcinoma (HCC) might originate from hepatic stem/progenitor cells.[9–12] A histologic study of clinical specimens also revealed that a substantial number of human HCC tissues have bipotential characteristics with coexpression of biliary and hepatocytic markers such as cytokeratin 7 (CK7), CK19, alpha-fetoprotein (AFP) and albumin.[13,14] Conversely, all cholangiocarcinoma tissues examined showed hepatocellular differentiation in part of the tumor and expression of hepatic progenitor cell markers.[15] Findings from a recent study also suggested that human HCC could arise as a consequence of the dysregulated proliferation of hepatic progenitor cells when the TGF-β and IL-6 signaling pathway was disrupted.[16]

Activation-induced cytidine deaminase (AID) can induce genetic alterations in human genome DNA sequences.[17,18] Under physiological condition, AID is expressed almost exclusively in B lymphocytes, and plays a critical role not only in class switch recombination but also in somatic hypermutation of immunoglobulin genes. We recently demonstrated that inflammatory stimulation triggers aberrant AID expression in epithelial cells and initiates and/or promotes oncogenic pathways by inducing genetic alterations in various tumor-related genes.[19,20] Indeed, AID expression is induced by proinflammatory cytokine stimulation and/or hepatitis C virus infection through NF-kB activation in hepatocytes,[21] and the resultant AID upregulation leads to the accumulation of somatic mutations in *TP53* and *c-MYC* genes, both of which are frequently mutated in human cancer tissues.[21,22] These findings suggest that aberrant AID production induced by chronic inflammation in the liver contributes to hepatocarcinogenesis via the accumulation of genetic aberrations in tumor-related genes.[23]

The fact that it usually takes over a year for AID transgenic (Tg) mice to accumulate the genetic aberrations required for carcinogenesis[24,25] prompted us to speculate that constitutive expression of AID in the cells with long life-span might possess the higher risk for malignant transformation compared to that in the cells with the limited life-span. Therefore, in our study, we took advantage of the AID-mediated stepwise genotoxicity that recapitulates human hepatitis-associated carcinogenesis to investigate whether liver cancer originates from fetal hepatic progenitor cells with constitutive AID expression. Accordingly, we separated hepatic progenitor cells enriched from the fetal liver of AID Tg mice followed by transplantation into recipient mice and examined whether recipient mice receiving AID-expressing hepatic progenitor cells develop liver tumors. Furthermore, to unveil the overall landscape of genetic alterations that accumulate in hepatic progenitor cells during the process of malignant transformation, we applied whole exome sequencing and determined the whole picture of genetic aberrations that accumulated in liver cancer cells originating from hepatic stem/progenitor cells.

Material and Methods

Animals

The "toxin-receptor mediated conditional cell knockout" mice, which are homozygous for the albumin enhancer/promoter driven-human heparin binding epidermal growth factor-like growth factor (hHB-EGF) alleles, achieve the specific and conditional ablation of hepatocytes under the treatment of diphtheria toxin (DT).[26] AID Tg mice were previously described.[24] All animals were maintained in a specific pathogen-free facility at the Kyoto University Faculty of Medicine. All animal experiments were approved by the ethics committee for animal experiments and performed under the Guidelines for Animal Experiments of Kyoto University.

Isolation of enriched hepatic progenitor cells, cell transplantation and administration of diphtheria toxin

Hepatic progenitor cells were obtained from the fetal liver of pregnant wild-type, AID Tg and green fluorescent protein (GFP) Tg mice on gestational day 13.5 and were enriched through sphere formation as previously described.[27] Briefly, after the digestion of fetal liver tissues using a 0.5% collagenase solution (Invitrogen, Carlsbad, CA), fetal liver cells were subjected to floating culture to form spheres in RPMI 1640 (Invitrogen) supplemented with 10% fetal calf serum. After 16 h incubation, the formed spheres were selected by gravity sedimentation and inoculated on Type-I collagen-coated culture plates (Asahi Glass, Chiba, Japan). After 24 h of incubation, floating hematopoietic cells were removed by washing and adhered cells were collected using trypsin-ethylenediaminetetraacetic acid (EDTA) solution (Sigma-Aldrich, St. Louis, MO) for 3 min. The dissociated cells were counted and suspended in a Ca^{2+}-free Hank's balanced salt solution (Invitrogen) with fetal calf serum at a density of 5.0

$\times 10^6$ cells/mL as the enriched hepatic progenitor cells. To characterize the enriched hepatic progenitor cells, expression levels of fetal liver stem/progenitor markers, including albumin, AFP, DLK1, CK19 and CD133 were examined using both immunohistochemistry and RT-PCR. In addition, the lack of expression of the hematopoietic cell marker CD45 in sphere-derived hepatic progenitor cells was also confirmed by both immunostaining and RT-PCR.

To achieve efficient engraftment of transplanted hepatic progenitor cells to livers of the recipient mice, we used TRECK mice as a liver-specific regeneration model.[26] TRECK mice express DT receptor under control of the albumin promoter, and treatment with DT selectively and efficiently ablates the hepatocytes, resulting in enhanced liver regeneration and efficient colonization of transplanted hepatic progenitor cells.[27] The enriched hepatic progenitor cells were transplanted into 7- to 9-week old TRECK mice using an intrasplenic approach.[27,28] We injected 0.2 mL of a cell suspension containing 1.0×10^6 hepatic progenitor cells. The DT was purified as described previously[26] and a total of 75 ng/kg DT was administered by intraperitoneal injection into recipient mice twice a week for 25 weeks from the day of cell transplantation.

Whole exome capture and massively-parallel sequencing

Massively-parallel sequencing was performed using the Illumina Genome Analyzer IIx (Illumina, San Diego, CA) as described.[29] End-repair of DNA fragments, addition of adenine to the 3' ends of DNA fragments, adaptor ligation and PCR amplification were performed according to the instructions. Exome capture was performed according to the NimbleGen Arrays Users Guide (Roche, Basal, Switzerland). The DNA library was hybridized to the custom designed NimbleGen Seq Cap arrays targeting a total of 17,089 genes, including 157,728 exons. These libraries were enriched independently using a minimal PCR amplification step of 18 cycles with Phusion High-Fidelity DNA polymerase. The concentration of enriched DNAs was measured by Quant-iT PicoGreen Reagent and Kits (Invitrogen) to make a working concentration of 10 nM. Cluster generation and sequencing was performed for 76 cycles on the Illumina Genome Analyzer IIx as described using the pair-end protocol and collecting 76 bases from each read.[29] The obtained images were analyzed and base-called using GA pipeline software version 1.4 with the default settings provided by Illumina. All sequence reads were deposited in the DNA Data Bank of Japan Sequence Read Archive; accession number DRA000601.

RNA preparation and hybridization to the microarray

Total RNA was extracted from adult mice (12-week old) liver tissues, bone marrow and the fetal liver at Day 13.5 of gestation using RNeasy Mini Kit (Qiagen, Valencia, CA). The details of the procedures for hybridization to the microarray were described previously.[30] RNA amplification and labeling were performed according to the manufacturer's instructions (Agilent Technologies, Palo Alto, CA). Array image acquisition and feature extraction were performed using an Agilent G2505C scanner with feature extraction software (Agilent Technologies). Microarray data were deposited in the GEO database; accession number GSE39213.

Genome Analyzer sequence data analysis and variant filtering.

Semiquantitative reverse transcription PCR and quantitative real-time genomic and reverse transcription-PCR

Histology and immunohistochemistry

Southern blot analysis

Statistical analysis

These procedures are described in Supporting Information Materials and Methods.[31–33]

Results

Enrichment of hepatic progenitor cells derived from fetal mouse liver

Enriched hepatic progenitor cells were obtained from the fetal liver of wild-type, AID Tg and GFP Tg mice through the formation of cell spheres, and the dissociated cells were cultured, counted and then transplanted into recipient mice (Fig. 1*a*). To characterize the sphere-derived hepatic cells used for the transplantation procedure, we first examined the expression of various marker genes in the fetal liver of wild-type mice. Immunohistochemistry revealed that expression of both the liver cell marker albumin and the hematopoietic cell marker CD45 were detectable in the fetal liver tissues (Fig. 1*b*). Cells expressing DLK1, a cell surface marker for hepatic stem/progenitor cells, comprised ~10% of the total cells of the fetal liver parenchyma (Supporting Information Fig. 2*a*). The enriched cell population specifically contained cells expressing the hepatocyte-lineage cell markers such as albumin and AFP, but no expression of CD45 was detectable in these sphere-forming cells (Fig. 1*c*). In addition, we confirmed that almost the entire enriched sphere-derived cell population expressed E-cadherin and DLK1, and a subset of those enriched cells expressed CK19 and CD133 (Supporting Information Fig. 2*b*). On the other hand, the floating cells that did not form spheres strongly expressed CD45 (Fig. 1*d*). RT-PCR also revealed that the sphere-forming cells prepared for the transplantation procedure expressed albumin, AFP, DLK1, CK19 and CD133 transcripts, but not CD45 (Fig. 1*e*). Similar results were obtained in the fetal liver of AID Tg mice (data not shown). These expression profiles of the collected sphere-derived cells were consistent with those found in previous studies[34] and indicated that the enriched cells derived from the fetal liver fully contained hepatic lineage progenitor cells.

Efficient engraftment of transplanted hepatic progenitor cells in the recipient liver

To enhance engraftment of the transplanted cells in the liver, we used TRECK mice as a liver-specific regeneration model.

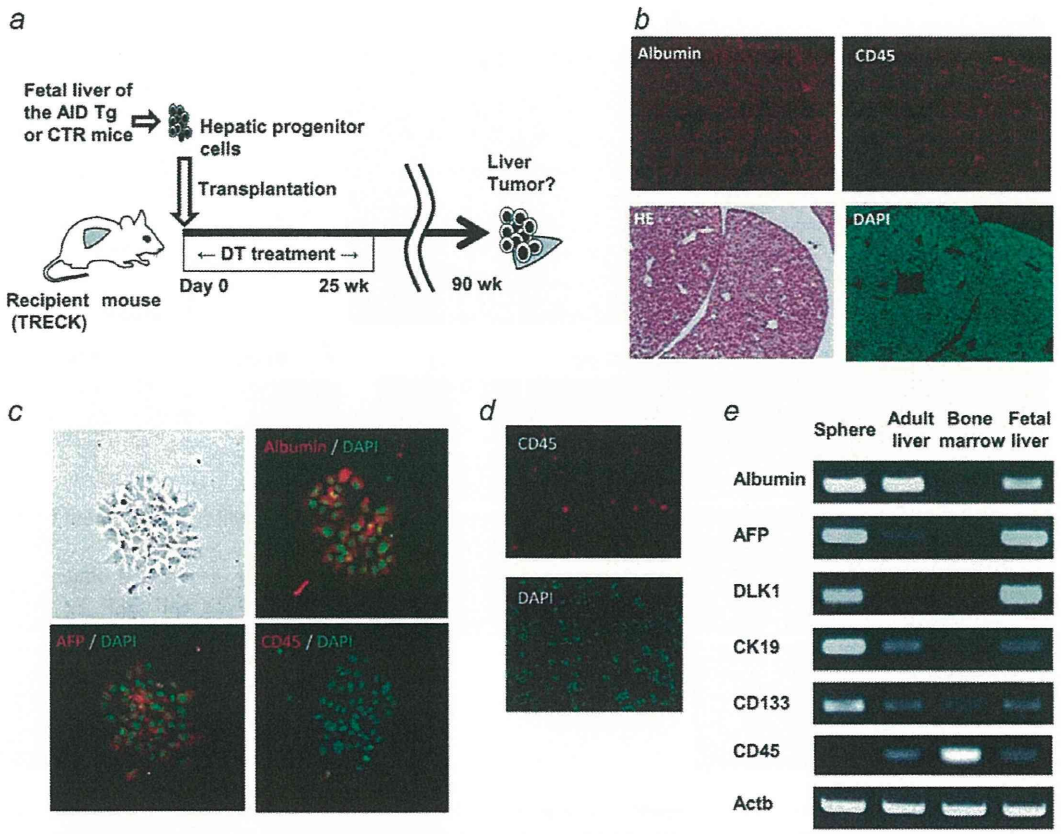

Figure 1. Enrichment of hepatic stem/progenitor cells from the fetal liver. (*a*) Schematic diagram showing the transplantation of the enriched hepatic stem/progenitor cells of AID Tg mice or control (CTR) mice into the recipient TRECK mice. DT was administered intraperitoneally twice a week to recipient (TRECK) mice for 25 weeks from the day of cell transplantation. The phenotypes were examined 90 weeks after transplantation. (*b*) Microscopic image (H&E staining) of the fetal liver tissues. Immunohistochemical staining for both the liver cell marker albumin and the hematopoietic cell marker CD45 are shown. (*c*) Immunohistochemical staining of the enriched cell population from the fetal liver via sphere formation for albumin, AFP and CD45. (*d*) Immunohistochemical staining of floating cells that did not form spheres for CD45. (*e*) Representative RT-PCR for the various phenotypic expression: albumin, AFP, DLK1, CK19, CD133, CD45 and control Actb (β-actin). Total RNA was extracted from the spheres of the enriched cell population from the fetal liver, adult liver tissue, bone marrow and fetal liver tissue.

These mice express hHB-EGF precursor, which functions as a DT receptor, under the control of an albumin promoter, and thus the hepatocytes of these mice are selectively ablated by the administration of DT.[26] We confirmed that the transcripts of hHB-EGF were specifically detectable in the liver of the TRECK mice (Fig. 2*a*), and immunohistochemistry also revealed that hHB-EGF protein expression was present in the TRECK mouse liver tissues (Fig. 2*b*). Serum alanine aminotransferase levels of a TRECK mouse were increased at 24 h after 75 ng/kg of DT administration, peaked at 48–72 h and subsequently returned to basal levels after 120 h (Fig. 2*c*). After repeated trials, we found that twice-weekly DT administration maintained the sublethal liver injury, resulting in the constitutive hepatic regeneration process. Under these experimental conditions, DT-mediated ablation of hepatocytes in TRECK mice resulted in the expansion of cells expressing E-cadherin, EpCAM and HNF4α accompanied by an increased number of the Ki67-positive cells, suggesting enhanced proliferation activity of hepatocyte-lineage cells including hepatic progenitor cells and mature hepatocytes in the TRECK liver tissues (Fig. 2*d*, and data not shown).

To examine the repopulation of the transplanted cells in the recipient liver, the hepatic progenitor cells of the GFP Tg fetal livers obtained in a similar way were introduced into the TRECK mice, followed by the repeated DT administration. At Day 7, the GFP-positive cells were observed as clusters, and at Day 30 the cluster of the GFP-positive cells was large enough to view macroscopically (Fig. 2*e*). Moreover, the cluster of hepatocytes derived from the transplanted GFP-positive enriched hepatic progenitor cells was detectable in the recipient liver even 90 days after the transplantation while no such cells were observed in the liver of mice

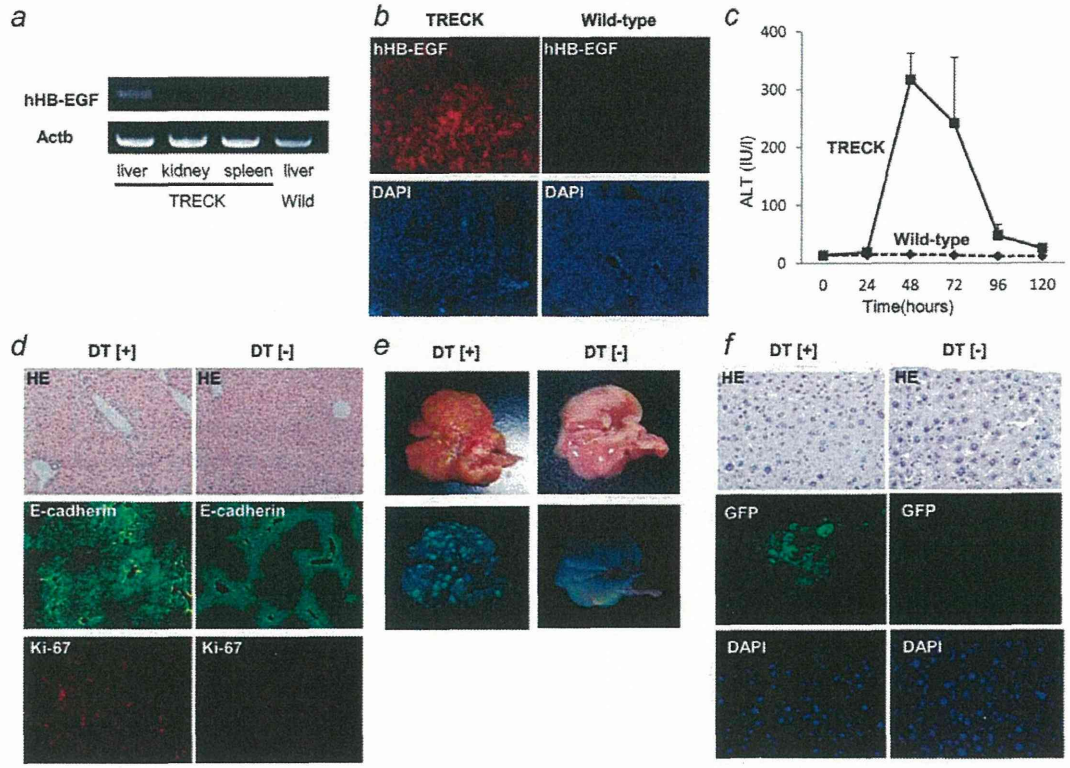

Figure 2. Efficient engraftment of the transplanted hepatic progenitor cells in the recipient liver. (*a*) The hHB-EGF expression in the liver, kidney and spleen of a TRECK mouse and the liver of a wild-type mouse determined by semiquantitative RT-PCR analysis. Upper, hHB-EGF expression; Lower, control Actb expression. (*b*) Immunohistochemical staining for human hHB-EGF in the liver of the TRECK and wild-type mice. Upper, hHB-EGF immunofluorescence; Lower, DAPI staining. (*c*) Time-course changes in ALT values of the TRECK and wild-type mice after the first DT administration. Vertical bars show SD. (*d*) Immunostaining analysis of liver tissue specimens of a TRECK mouse with (DT [+]) or without (DT [−]) DT administration. Upper, H&E staining; Middle, E-cadherin immunofluorescence; Lower, Ki-67 immunofluorescence. (*e*) Macroscopic image of a representative liver receiving GFP-positive hepatic progenitor cells at 30 days after transplantation. (F) Histologic analysis of liver tissue specimens receiving GFP-positive hepatic progenitor cells at 90 days after transplantation. Upper, H&E staining; Middle, GFP immunofluorescence; Lower, DAPI staining.

without DT administration (Fig. 2*f*). These findings indicated that the transplanted cells efficiently engrafted and continued to proliferate in the recipient livers treated with DT as time progressed.

Transplanted hepatic progenitor cells with constitutive AID expression progressed to liver cancers

Next, the enriched hepatic progenitor cells from AID Tg mice were transplanted into 13 recipient (TRECK) mice, and the DT was administered to the recipient mice for 25 weeks. Two mice died in a week after transplantation, while the remaining 11 mice were viable and thus subjected to phenotypic analyses. We found that liver tumors developed in 7 of 11 (63.6%) recipient mice that received the enriched hepatic progenitor cells of the AID Tg mice 90 week after cell transplantation (Fig. 3*a*). Among them, four mice developed multiple tumors and three developed a single large nodule. On the other hand, none of the 13 recipient mice receiving hepatic progenitor cells from wild-type or GFP Tg mice showed tumorigenesis during the same observation period, while only one mouse developed a tumor with the characteristics of lipoma. Moreover, all the five recipient mice examined that received the mature hepatocytes of adult AID Tg mice at 6 months of age showed no phenotypic changes in the liver tissues. Histologic examination revealed that all the tumors examined showed the characteristics of well-to-moderately differentiated HCC. Interestingly, one tumor showed not only the enhanced AFP expression but also the ductal formation of tumor cells accompanied by the expression of CK19, indicating the features of intrahepatic cholangiocarcinoma (ICC) (Fig. 3*b*, upper and middle panel). In addition, partial positivity for MUC1 immunostaining in the tumor indicated that the tumor contained the mucin-producing area (data not shown). On the other hand, no histologic changes were observed in the non-tumorous region of liver tissues receiving the AID-expressing hepatic progenitor cells (Fig. 3*b*, lower panel).